ANNALES
UNIVERSITATIS MARIAE CURIE-SKŁODOWSKA
LUBLIN – POLONIA

VOL. LVII, 1 SECTIO AA 2002

The real space renormalization group and lattice gas model

A. Tarasenko and L. Jastrabik
Institute of Physics, Academy of Sciences of the Czech Republic, Na Slovance 2, 182 21, Prague 8, Czech Republic

The article presents a brief survey of application of the real space renormalization group to investigation of the thermodynamic properties of Ising-like and lattice-gas two dimensional systems. A number of RSRG transformations for a square lattice and their properties have been compiled together.
It is shown that the precision of the RSRG method strongly depends not only on the size of the blocks used in the RSRG transformations, but also on its symmetry and composition. In general, the accuracy of the RSRG method increases with the number of sites in the block. But the most accurate results have been obtained for blocks of average sizes having all symmetry elements and optimal composition.
We present results of the RSRG calculations of many thermodynamic quantities: phase diagrams, adsorption isotherms, spontaneous magnetization, coverage dependencies of the pair correlation function for the nearest neighbor particles, the isothermal susceptibility, tracer, jump and chemical diffusion coefficients. The RSRG data are compared with the well-known exact expressions and results obtained by Monte Carlo simulations. The coincidence between the exact, numerical and RSRG data is surprisingly good.

1. INTRODUCTION

The investigations of surface phenomena have been attracting a great deal of interest due to their apparent importance for catalysis, protection from corrosion, fast miniaturization of the solid state electronic components and devices. The outstandingly successful progress in this vast field have been achieved to the large extent due to the very intensive and extensive theoretical studies [1], and computer simulations [2].

The theoretical description of the various surface phenomena observed in experimental studies presents a considerable challenge, since it not only has to include the interaction of the adsorbed particles with the underlying substrate but also the lateral particle-particle interactions in a two-dimensional layer. Substantial insight into surface processes has been achieved by the developing of simple lattice models based on short-range lateral adsorbate interactions. The statistical study of systems of strongly interacting particles is quite difficult. It is therefore not surprising that a great deal of effort has been devoted into developing the simplest possible models, which have the advantage of exact treatment, despite their oversimplification of real phenomena. Some simple lattice models have been proposed in order to investigate adsorption and diffusion processes on crystal surfaces. In the majority of models the particles occupy the equivalent lattice sites formed by the minima of the potential relief of the crystal surface. Usually the minima are arranged in a two-dimensional lattice having definite symmetry, for example, honeycomb, square or triangular. The position of any particle is strictly determined by a position of the lattice site, which this particle occupies. Therefore, each cell can be in two possible states: occupied by a particle or empty. Then any microstate of a system can be described by a set of occupation number $n_i = 1,2...,N$, where i labels the lattice sites and

$$n_i = \begin{cases} 1, & \text{if site } i \text{ is occupied} \\ 0, & \text{if site } i \text{ is empty} \end{cases} \tag{1}$$

Lattice gas model works rather good for strongly adsorbed particles. It means that the depth of the potential minima, ε, must be large relative to the thermal energy, $k_B T$, and characteristic lateral particle-particle interaction energy. In this case the adsorbed particles will almost always be located in the minima, jumping from time to time to the nearest empty sites.

The Hamiltonian of the system, accounting for the pair lateral interaction between the nearest neighbor (nn) particles only, is

$$H_a = -\varepsilon N_a + \varphi \sum_{nn} n_i n_j \tag{2}$$

where $N_a = \sum_i n_i$ is the number of particles, φ is the interaction energy and symbol nn means that summation is performed over all lattice bonds just once.
In the thermodynamic equilibrium the system is described by the statistical operator,

$$\rho = Q^{-1} \exp\left(\frac{\mu N_a - H_a}{k_B T} \right) \tag{3}$$

where μ is the chemical potential of the particles; Q is the grand partition function.

$$Q = \sum_{\{n_i\}} \exp\left(\frac{\mu N_a - H_a}{k_B T} \right) \tag{4}$$

The summation in eq. (4) is carried out over all 2^N configurations of the particle system.

The value of any thermodynamic quantity $\langle A \rangle$ is obtained by the averaging of the corresponding operator $A(n_i)$ with the statistical operator, ρ, over all particle configurations

$$\langle A \rangle = \sum_{\{n_i\}} A(n_i) \rho \tag{5}$$

For example, the surface coverage θ is the averaged value of the simplest operator n_i

$$\theta = \langle n_i \rangle \tag{6}$$

For practical purposes better to use the logarithm of the grand partition function or free energy (per site), f , which we define as follows

$$F = k_B T N^{-1} \ln Q \tag{7}$$

Then, the entropy S and internal energy U have the following forms

$$U = k_B T \frac{\partial f}{\partial T} - f \,, \qquad S = \frac{\partial f}{\partial T} \tag{7}$$

All thermodynamic quantities can be expressed via the corresponding derivatives of the free energy over its arguments: the chemical potential μ and temperature T .

2. BASICS OF SURFACE DIFFUSION

Surface diffusion of adsorbates on metal and alloy surfaces has become an important subject of surface science [3,4]. The detailed comprehension of surface diffusion is one of the key steps in understanding (and controlling) many interesting surface phenomena such as adsorption, desorption, catalytic

reactions, melting, roughening, and crystal and film growth. Despite the widespread availability of experimental techniques for the measurement of surface diffusion coefficients, a lot more work remains to be done for a complete understanding of this phenomenon. In many cases the interpretation of experimental surface diffusion data has been rather tedious, especially in heterogeneous systems and systems undergoing phase transitions. Therefore, many different theoretical and numerical methods such as mean-field [5-8], Bethe-Peierls [9], real-space renormalization group [10-14], and Monte Carlo [15-18] methods have been used in order to describe the surface diffusion phenomenon.

In this section we give the basic definitions needed to understand the computational results, which will be described in the following parts of this paper.

Some diffusion coefficients had been defined in order to describe the particle migration. Conceptually the simplest diffusion coefficient is a single particle or tracer diffusion coefficient, D_t. The surface tracer diffusion coefficient, D_t, describes the random walk of a tagged single particle

$$D_t = \lim_{t\to\infty} \frac{1}{2dt} \left\langle \left| \vec{r_i}(t) - \vec{r_i}(0) \right|^2 \right\rangle \tag{8}$$

where d is the system dimension, (in the case of surface diffusion $d = 2$); the vector $\vec{r}(t)$ determines the position of a tagged particle at time t, and $\left\langle (\vec{r_i}(t) - \vec{r_i}(0))^2 \right\rangle$ is its mean square displacement.

The jump diffusion coefficient, D_j, is a many particle diffusion coefficient describing the asymptotic behavior of the mean square displacement of the system center of mass $\overrightarrow{R_c}(t)$. The jump diffusion coefficient is defined in the following way

$$D_t = \lim_{t\to\infty} \frac{1}{2dN_a t} \left\langle \left[\overrightarrow{R_c}(t) - \overrightarrow{R_c}(0) \right]^2 \right\rangle, \text{ where } \overrightarrow{R_c}(t) = \sum_{i=1}^{N} n_i \vec{r_i}(t) \tag{9}$$

The definitions for D_t and D_j are quite suitable for MC simulations as the desired quantities are expressed in terms of the directly measured variables.

The chemical diffusion coefficient is determined by the Fick's first law, which constitutes a relationship between the flux of particles $\vec{J}(\vec{r},t)$ and the gradient of the particle coverage $\theta(\vec{r},t)$

$$\vec{J}(\vec{r},t) = -D_c \vec{\nabla}\theta(\vec{r},t) \tag{10}$$

We consider that particle migration proceeds by the nn uncorrelated jumps only. A particle on site i can jump to one of its nn sites if the destination is empty. The activated particle must surmount the potential barrier E_{if} between the initial site i and the final site *f*. For noninteracting Langmuir lattice gas the potential barrier is a constant throughout the lattice. We set the value is equal to the site depth ε. In case of interacting lattice gas the activation energy of jumps is affected by the presence of adjacent particles. We assume that the interactions influence the minima of the periodic potential. In order to obtain the suitable expression for the chemical diffusion coefficient we have used the local equilibrium approximation. The interested reader is referred to Refs. [9,11] for a detailed description of this approach. In this approximation the chemical diffusion coefficient, D_c, has the following simple form

$$D_c = D_0 \exp(\mu / k_B T) P_{00} / \chi_T \tag{11}$$

Here

$$D_0 = z\nu a^2 / 4$$

is the diffusion coefficient of noninteracting particles; $\nu \propto \exp(-\varepsilon / k_B T)$ is the jump frequency of a particle over the surface; z is the coordination number of the lattice, $z = 3,4,6$ for the honeycomb, square and triangular lattices, correspondingly.

The correlation function P_{00} is the probability to find two empty nn lattice sites

$$P_{00} = \langle (1-n_i)(1-n_j) \rangle \tag{12}$$

where $\left|\vec{r_i} - \vec{r_j}\right| = a$; a is the lattice constant.

The mean square surface coverage fluctuations, or isothermal susceptibility

$$\chi_T = N^{-1}\sum_{ij}\left\langle (n_i-\theta)(n_j-\theta)\right\rangle \tag{13}$$

is the second derivative of the free energy over the chemical potential. There is a simple relation between the jump and chemical diffusion coefficients: $D_j = D_c\chi_T/\theta$. For the Langmuir lattice gas the relations between the diffusion coefficients are following

$$D_t = D_j = (1-\theta)D_c \tag{14}$$

One can express easily all quantities entering eq. (11) via the following first and second derivatives of the free energy f over the chemical potential, μ, and the pair interaction parameter, φ:

$$\begin{aligned} \theta &= \frac{\partial f}{\partial \mu} \qquad \left\langle n_0 n_1\right\rangle = -\frac{2}{z}\frac{\partial f}{\partial \varphi} \\ \chi_T &= \frac{\partial^2 f}{\partial \mu^2} \quad P_{00} = 1-2\theta+\left\langle n_0 n_1\right\rangle \end{aligned} \tag{15}$$

The calculation of the free energy and its derivatives requires some approximate methods. Even for the simplest lattice gas model with the *nn* interaction only, the problem remains too complex to be solved exactly. The well-known Onsager's solution for a 2D Ising model was obtained in zero magnetic field, which is equivalent to half monolayer particle coverage, $\theta = 0.5$ [19].

In the following Section we will briefly outline the renormalization group approach used for this purpose.

3. REAL SPACE RENORMALIZATION GROUP

In 1971 Kenneth Wilson introduced the concept of renormalization to investigation of critical phenomena in systems with continuous spins [20,21]. The renormalization proceeds in the reciprocal space and results are obtained as series of the 'small' parameter $\varepsilon = 4-d$, where d is the dimensionality of the system. Obviously that the two-dimensional systems should be treated in another way, which was developed in 1974 by Niemeijer and van Leeuwen [22,23] and by Nauenberg and Nienhuis [24,25]. They suggested to carry out the renormalization transformations in the real space. They had used the intuitive ideas of Kadanoff about the mechanism of reduction of relevant degrees of freedom near the critical point [26,27]. In their approach the original

lattice is divided into cells or blocks and the effective renormalized interaction between blocks is determined via the original Hamiltonian interaction parameters. The method was referred to as the real space renormalization group (RSRG). Subbaswamy and Mahan extended the RSRG approach to the Ising spin system with non-zero magnetic field and lattice gas models [28,29]. A further development of the RSRG method was made by Schick, Walker and Wortis, which introduced the so-called sublattice renormalization transformation [30,31]. In their approach the lattice is divided into sublattices two, three or more. Each block contains sites in the one sublattice only. Usually the blocks in such transformations interpenetrate each other, so are different that the blocks in the previous (cell) RSRG transformations.

It should be noted that the renormalization group approach has provided an effective calculational tool for numerical estimations for various critical parameters.

We start with the Ising model in the magnetic field. In the Ising model any i th site contains spin, $s_i \pm 1$. It is well known that the lattice-gas model with the nn pair interaction only is equivalent to the Ising spin model with an external magnetic field. Empty sites are equivalent to $s = -1$, and full sites to $s = 1$. There is a one to one correspondence between the occupation numbers and site spins: $s_i = 2n_i - 1$. Using this relation one can obtain easily the reduced Hamiltonian eq. (4) in the spin representation

$$(\mu N_a - H_a)/k_B T \equiv H(s) = h\sum_i^N s_i + p\sum_{nn} s_i s_j + Nc \tag{16}$$

Here

$$h = (\mu + \varepsilon - z\varphi/2)/2k_B T\ ,\ p = -\varphi/4k_B T\ ,\ c = (\mu + \varepsilon - z\varphi/4)2k_B T$$

The chemical potential of the particles is equivalent to the external magnetic field. Although the lattice gas model, eq. (2), and Ising spin model, eq. (16), are fully equivalent, we prefer to use the spin representation in the following because of its apparent symmetry with respect to the sign of the magnetic field (the symmetry is rather useful for the calculations of the thermodynamic quantities). However, we will refer to lattice gas terms where this seems to be more transparent.

It is very important to choose the form and size of blocks for a good RSRG transformation. As was mentioned above, the whole lattice is divided into blocks (or cells) of L sites each. All blocks together must form a new lattice of the same symmetry with the lattice constant $\sqrt{L}a$. A block spin $S_n = \pm 1$ is assigned to each block. We note that two values of the block spin S_n

corresponds to 2^L site spin configurations (since L spins are combined to form a block). Using some rule(s) one must distribute the configurations into the domains, corresponding to the definite values of the block spin. For blocks with odd number of the site spins the block spin is usually determined by the so-called majority rule (MR) [32]

$$S_n = \text{sign}\left(\sum_{i=1}^{L} s_i\right) \tag{17}$$

with

$$\text{sign}(x) = \begin{cases} +1, & \text{if } x > 0 \\ -1, & \text{if } x < 0 \end{cases}$$

For even L an additional rule must be introduced in order to assign a definite value of the block spin to any given configuration having zero sum of site spins. In any case an obvious condition must be fulfilled: if the site spin configuration $\{s_1, s_2, ..., s_L\}$ is assigned a block spin value S_n, then the configuration $\{-s_1, -s_2, ..., -s_L\}$, is assigned the opposite value, $-S_n$.

The RSRG transformation of the spin system allows the reduction of the number of independent variables, i.e. the transition from the set of N site spins $\{s_i\}$ to the set of N/L block spins $\{S_n\}$. The transformation can be written as a partial summation of the grand partition function

$$\exp[H(S) + Lg] = \sum_{\{s\}} \exp[H(s)] \tag{18}$$

where $H(S)$ is the renormalized Hamiltonian of the block spin system, g is the so-called self-energy term, which plays an important role in the RSRG method. The summation is carried out over the site spin configurations $\{s_i\}$, which keep the values of the block spins $\{S_n\}$ fixed.

The main idea of any RSRG transformation is that the result of the summation should have the same form as the original Hamiltonian eq. (16) plus insignificant terms, which affect weakly the critical behavior of the system. After the RSRG iteration the Hamiltonian, $H(S)$, must have the same form as the original eq. (16) with another, in general case, values of the Hamiltonian parameters: magnetic field, h_1, and pair interaction parameter, p_1. Then any RSRG transformation can be considered as a jump of the system in the parametric plane

$$\overrightarrow{\mathfrak{R}_1} = \hat{\mathfrak{I}}\,\overrightarrow{\mathfrak{R}} \tag{19}$$

Here $\hat{\Im}$ is the operator of the RSRG transformation, translating the system from the initial point $\vec{\Re}$ to a new point $\vec{\Re}_1$. The successive RSRG transformations cause flow of the Hamiltonian parameters along some trajectory in the plane (h, p). The form of the trajectory depends on the starting point and the RSRG transformation used for calculations. The analysis of the trajectories reveals interesting features of the RSRG transformations.

Any RSRG transformation does not change the state of the system. If one applies the RSRG transformation to a disordered (ordered) state, the system will stay in the same disordered (ordered) state after any number of the successive RSRG transformations. If one start just below the critical line $T_c(h)$ (system is in ordered phase), subsequent RSRG iterations flow the system along the boundary. Then the trajectory diverges from the line towards the origin point $1/|p| = h/|p| = 0$ (see Figure 1). An initial point just above the boundary leads towards the infinite magnetic fields $h/|p| \to \pm\infty$. It gives a rather simple and effective method of determining the phase boundaries for the Ising antiferromagnet in the external magnetic field (which equivalent to the phase boundary between the ordered and disordered phases for the lattice gas with repulsive lateral interaction). The location of the phase boundary by this method is very fast and reliable.

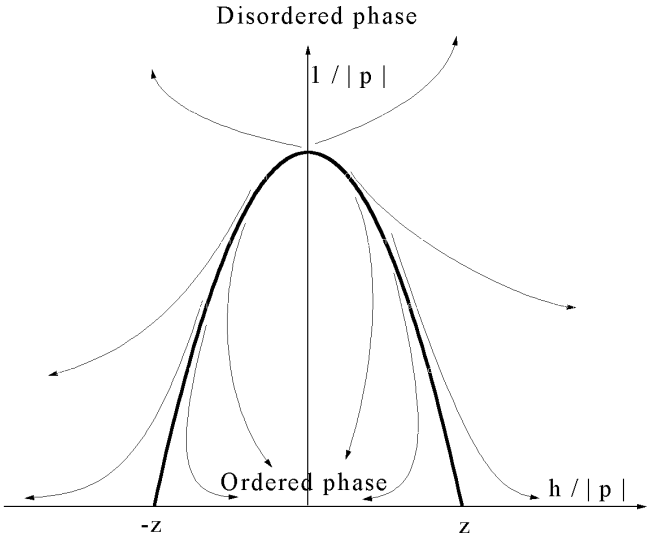

Fig. 1. Schematic view of the phase diagram for the Ising antiferromagnet (thick line) plotted in the dimensionless coordinates "magnetic field – temperature". The RSRG trajectories shown as thin lines. The endpoints of the phase diagram correspond to the critical value of the magnetic field $h = \pm z\,|p|$, separating ferromagnetic and antiferromagnetic ordered ground states

As was shown by Nauenberg and Nienhuis [24], the free energy of the system can be evaluated in the series of sequential RSRG transformations of the original Hamiltonian. To get the necessary expression we carry out the summation of eq. (18) over the block spin configurations. The logarithm of the equation has the form

$$k_B T \ln \sum_{\{S_n\}} \exp[H(S)] = \frac{N}{L} f(h_1, p_1) + k_B T N g(h, p) \tag{20}$$

The left-hand side (LHS) is expressed as

$$k_B T \ln \sum_{\{S_n\}} \sum_{\{s_i\}} \exp H(s) = N f(h, p) \tag{21}$$

Then, one arrives to the following renormalization equation for the free energy

$$f(h, p) = k_B T g(h, p) + L^{-1} f(h_1, p_1) \tag{22}$$

Successive iterations of the RSRG transformation leads to the desired result

$$f(h, p) = k_B T \left[g(h, p) + L^{-1} \left(g(h_1, p_1) + L^{-1} (g(h_2, p_2) + \ldots) \right) \right] =$$

$$= k_B T \sum_{m=0}^{n-1} L^{-m} g(h_m, p_m) + L^{-n} f(h_n, p_n) \tag{23}$$

There is no problem in calculation of the last term in the RHS of eq. (23). The renormalized parameters h_n and p_n monotonically grow or decrease

$$\begin{aligned} &\lim_{n \to \infty} h_n \to \pm\infty \text{ or } 0 \\ &\lim_{n \to \infty} p_n \to \pm\infty \text{ or } 0 \end{aligned} \tag{24}$$

Therefore the free energy $f(h_n, p_n)$ can be calculated in a direct way (in most cases this term becomes negligible after some iterations) [33].

The most important property of the RSRG transformation is the existence of fixed points. The fixed points are determined by the conditions $\overrightarrow{\Re_1} = \vec{\Re}$. The unstable fixed points of the system correspond to the critical points of the Hamiltonian eq. (16). In the close vicinity of the fixed point $\overrightarrow{\Re_c}$ the behavior of

the system is governed by the linearized matrix of the RSRG transformation, $\overrightarrow{\Im_c}$

$$\overrightarrow{\Re_1} - \overrightarrow{\Re_c} = \vec{\Im}\left(\vec{\Re} - \overrightarrow{\Re_c}\right) \tag{25}$$

Here

$$\overrightarrow{\Im_c} = \begin{pmatrix} \partial h_1 / \partial h & \partial p_1 / \partial p \\ \partial p_1 / \partial h & \partial p_1 / \partial p \end{pmatrix}$$

where all derivatives are calculated at the critical point.

The eigenvalues, λ_i ($i = 1,2$), of the matrix, $\overrightarrow{\Im_c}$, (which are assumed to be real and positive) control the critical behavior of the free energy and its derivatives over the magnetic field and interaction parameter. The singular behavior of the thermodynamic quantities is determined by the RSRG critical exponents, y_i

$$y_i = 2 \ln \lambda_i / \ln L$$

Only the relevant ($y_i > 0$) eigenvalues lead to the non-analytical critical behavior of the thermodynamic quantities.

The following simple analysis should help reader to understand the above mentioned statements. Suppose that the linearized matrix, $\overrightarrow{\Im_c}$, is diagonalized by the proper shift and rotation of the coordinate axes (h, p). The new coordinates are denoted as (κ, η) and fixed point corresponds to the origin of the new coordinate system $\kappa_c = \eta_c = 0$. Let us consider the free energy in a close vicinity of a fixed point

$$f(\kappa, \eta) = \sum_{m=0}^{\infty} L^{-m} g(\lambda_1^m \kappa, \lambda_2^m \eta) \tag{26}$$

If any of the eigenvalues exceeds 1 (for example, $\lambda_1 > 1$), then exists an integer n satisfying the following conditions

$$\lambda_1^{n-1} < L \text{, and } \lambda_1^n \geq L \tag{27}$$

and the nth derivative of the free energy, $f(\kappa,0)$, over κ

$$f_{\kappa}^{(n)}(\kappa) \equiv \frac{\partial^n}{\partial \kappa^n} f(\kappa,0) = \sum_{m=0}^{\infty} \left(\frac{\lambda_1^n}{L} \right)^m g_1^{(n)}\left(\lambda_1^m \kappa, 0\right) \tag{28}$$

will be divergent as $\kappa \to 0$.

For the further analysis suppose, that the asymptotic singular behavior of the nth derivative of the free energy $f_{\kappa}^{(n)}$ can be expressed as following

$$f_{\kappa}^{(n)}(\kappa) \propto A\kappa^{y} + \text{less singular terms} \tag{29}$$

Then we calculate the nth derivative after the first RSRG transformation

$$f^{(n)}(\lambda_1 \kappa) = \sum_{m=0}^{\infty} \left(\frac{\lambda_1^n}{L} \right)^m g_1^{(n)}\left(\lambda_1^{m+1} \kappa\right) =$$

$$= \frac{L}{\lambda_1^n} \sum_{m=1}^{\infty} \left(\frac{\lambda_1^n}{L} \right)^m g_1^{(n)}\left(\lambda_1^m \kappa\right) = \frac{L}{\lambda_1^n} \left[f_{\kappa}^{(n)}(\kappa) - g_{\kappa}^{(n)}(\kappa) \right] \tag{30}$$

Using Eqs. (29-30), and taking into account that g is a smooth function without singularity, one can obtain the exponent y as

$$y = \frac{\ln L}{\ln \lambda_1} - n = 2/y_1 - n \tag{31}$$

It should be noted that $y \le 0$ as $\lambda_1^n \ge L$ (or $y_1 \ge n/2$). If $y = 0$, eq.(30) reads as follows

$$\lim_{\kappa \to 0} \left[f_{\kappa}^{(n)}(\lambda_1 \kappa) - f_{\kappa}^{(n)}(\kappa) \right] = g_{\kappa}^{(n)}(0) \neq 0 \tag{32}$$

In this case the singular part of the nth derivative is proportional to the $\ln \kappa$. It is known from the Onsager solution that the second derivative of the free energy over the temperature (or pair interaction parameter) has the logarithmic divergence in the critical point. Then the exact RSRG transformation should have the corresponding critical exponent equal to one or $\lambda = \sqrt{L}$. Usually, all RSRG transformations have the so-called temperature-like, relevant eigenvalue (with exponent y_T), and the field-like relevant eigenvalue (with exponent y_h).

The relations of the thermodynamic critical exponents and the two RSRG exponents y_T and y_h are given by the following set of equations [32]

$$\begin{aligned} \alpha &= 2(1-y_T^{-1}) \qquad \beta = (2-y_h)/y_T \\ \gamma &= 2(y_h-1)/y_T \qquad \delta = y_h/(2-y_h) \end{aligned} \tag{33}$$

Here the critical exponents α, β, γ, δ characterize the singular behavior of the specific heat, spontaneous magnetization, magnetic susceptibility and the response to an external magnetic field, respectively. The exact values for the Ising spin model are well known: $\alpha = 0$, $\beta = 1/8$, $\gamma = 7/4$ and $\delta = 15$. The values correspond to the following exact values of the RSRG exponents: $y_T = 1$ and $y_h = 15/8$ [34].

In order to carry out the summation in eq. (18) some further approximation should be used. In the framework of the RSRG approach, one usually employs periodic boundary conditions. It is assumed that the whole lattice is given by the periodic continuation of a small cluster of blocks. We consider here the smallest possible cluster of two blocks for the honeycomb and square symmetries. The renormalized Hamiltonian, $H(S)$, has the same form as the original eq. (16)

$$h_1(S_1+S_2) + z_1 S_1 S_2 + 2Lg = \ln \sum_{\{s\}} \exp[H(s)] \equiv \Psi(S_1, S_2) \tag{34}$$

Here the summation is carried out over all possible configurations $\{s_i\}$ keeping the values of the block spins $S_{1,2}$ fixed. The solution of the equation is the system of renormalization equations

$$\begin{aligned} h_1(h,p) &= (\Psi_{++} - \Psi_{--})/4 \\ p_1(h,p) &= (\Psi_{++} + \Psi_{--} - 2\Psi_{+-})/16z \\ g(h,p) &= (\Psi_{++} + \Psi_{--} + 2\Psi_{+-})/8L \end{aligned} \tag{35}$$

Here $\Psi_{\pm\pm} = \Psi(S_1, S_2)$ represents the RHS of eq. (34) with definite values of the block spins S_1 and S_2. Due to the symmetry of the Hamiltonian eq. (16) the functions $\Psi_{\pm\pm}$ have the following properties:

$$\begin{aligned} \Psi_{+-}(h,p) &= \Psi_{-+}(h,p) \\ \Psi_{+-}(h,p) &= \Psi_{+-}(-h,p) \\ \Psi_{--}(h,p) &= \Psi_{++}(-h,p) \end{aligned}$$

The block spin functions $\Psi_{\pm\pm}$ depend strongly on the size and the symmetry of the blocks. The calculation of these functions is the most time consuming part of the RSRG calculations. Therefore, effective algorithms are very important for the fast handling of the RSRG transformations with huge blocks, containing many site spins.

In the next Sections we will consider the RSRG transformations for the square lattice.

4. RSRG TRANSFORMATIONS

We will consider ferromagnetic (F) and antiferromagnetic (AF) interactions between the site spins s_i (in the lattice gas terminology these interactions represent attraction and repulsion between the adjacent particles, respectively). The exact critical values of the interaction parameter p^* for the F and AF interactions for the square Ising model was determined at first by Kramers and Wannier [35]

$$p_F^* = -p_{AF}^* = \frac{1}{2}\ln\left(1+\sqrt{2}\right) \approx 0.4406868 \tag{36}$$

We employ periodic boundary conditions in order to carry out the RSRG transformations. It is assumed that the whole lattice is given by the periodic continuation of a small cluster of blocks. The smallest possible cluster consists of two blocks. We have investigated a large number of RSRG transformations on the square lattice with blocks of different symmetries and sizes varying from 3 to 27 lattice sites. The RSRG blocks are shown in Figures 2 and 3, and their critical properties are compiled in Tables 1 and 3 for the F and AF interaction, respectively.

For all RSRG transformations we have calculated values of the pair interaction parameter in the ferromagnetic and antiferromagnetic regions, p_F and p_{AF}, and corresponding relative errors

$$\varepsilon_{F,AF} \equiv \left| p_{F,AF} - p^* \right| / p^* \cdot 100\% \tag{37}$$

We calculated critical exponents, y_h and y_T, and also entropy S_c and internal energy U_c (at the ferromagnetic critical point). The best estimates for these quantities had been obtained from the high-temperature series [36]:

$$S_c = 0.30647 k_B, \qquad U_c = -0.62323 k_B T \tag{38}$$

Tab.1. Compilation of the ferromagnetic critical values for the different clusters on a square lattice. p_F , ε_F , $y_{h,T}$ are the critical values of the pair interaction parameter, the relative error and critical exponents; S_c and U_c are the critical entropy and internal energy calculated in the F critical point

#	Cluster	p_F	ε_F %	y_h	y_T	S_c / k_B	$-U_c / k_B T$
	Exact	0.44069		1.875	1.0	0.3065	0.6232
1	3 × 2	0.56429	28.05	1.923	0.653	0.159	0.994
2	4 × 2	0.52874	19.98	1.942	0.729	0.151	0.929
3	4 × 2	0.42501	3.557	1.839	0.753	0.318	0.589
4	4 × 2S	0.42501	3.557	1.839	0.753	0.318	0.589
5	4 × 2S	0.42501	3.557	1.839	0.753	0.318	0.589
6	5 × 2	0.48223	9.427	1.911	0.763	0.216	0.782
7	5 × 2S	0.36037	18.23	1.695	0.613	0.456	0.367
8	6 × 2	0.38133	13.47	1.746	0.651	0.415	0.433
9	8 × 2	0.37864	14.08	1.722	0.640	0.432	0.414
10	8 × 2	0.38103	13.54	1.729	0.617	0.424	0.425
11	9 × 2	0.40962	7.049	1.806	0.753	0.365	0.520
12	9 × 2	0.45335	2.872	1.887	0.830	0.268	0.682
13	9 × 2S	0.35965	18.39	1.663	0.612	0.478	0.346
14	10 × 2	0.38889	11.75	1.734	0.642	0.415	0.445
15	11 × 2	0.43390	1.541	1.853	0.813	0.313	0.608
16	12 × 2	0.39604	10.13	1.736	0.645	0.405	0.465
17	12 × 2	0.41728	5.311	1.818	0.749	0.350	0.547
18	13 × 2	0.40319	8.509	1.777	0.712	0.388	0.490
19	13 × 2	0.39256	10.92	1.744	0.704	0.416	0.449
20	13 × 2	0.40319	8.509	1.777	0.712	0.388	0.490
21	13 × 2	0.42145	4.365	1.825	0.774	0.343	0.559
22	13 × 2	0.45326	2.853	1.887	0.832	0.268	0.682
23	13 × 2	0.44757	1.561	1.878	0.824	0.281	0.660
24	13 × 2S	0.36744	16.62	1.658	0.597	0.472	0.364
25	14 × 2	0.40705	7.632	1.750	0.635	0.383	0.503
26	14 × 2	0.39232	10.98	1.731	0.645	0.415	0.449
27	15 × 2	0.44173	0.236	1.871	0.852	0.295	0.636
28	16 × 2	0.41493	5.844	1.756	0.630	0.368	0.529
29	16 × 2	0.42975	2.481	1.845	0.793	0.323	0.591
30	17 × 2	0.43312	1.716	1.852	0.826	0.317	0.602
31	17 × 2	0.43710	0.813	1.861	0.832	0.307	0.618
32	17 × 2	0.43710	0.813	1.861	0.832	0.307	0.618
33	17 × 2	0.44540	1.069	1.877	0.850	0.287	0.651
34	17 × 2	0.43710	0.813	1.861	0.832	0.307	0.618
35	17 × 2	0.41346	6.179	1.802	0.777	0.368	0.523
36	17 × 2S	0.36808	16.48	1.642	0.590	0.478	0.359
37	17 × 2	0.39312	10.79	1.737	0.689	0.419	0.446
38	17 × 2	0.44012	0.128	1.867	0.840	0.299	0.630
39	17 × 2	0.44059	0.021	1.850	0.754	0.301	0.630
40	18 × 2	0.42467	3.634	1.768	0.612	0.347	0.564

Tab. 2. Continuation of the Table 1

#	Cluster	p_F	ε_F %	y_h	y_T	S_c / k_B	$-U_c / k_B T$
	Exact	0.44069		1.875	1.0	0.3065	0.6232
41	18 × 2	0.42918	2.611	1.842	0.792	0.326	0.587
42	18 × 2	0.42004	4.686	1.818	0.787	0.351	0.549
43	20 × 2	0.43144	2.098	1.772	0.605	0.334	0.587
44	20 × 2	0.43221	1.924	1.850	0.816	0.320	0.598
45	20 × 2	0.41318	6.241	1.756	0.623	0.372	0.522
46	21 × 2	0.43732	0.764	1.859	0.848	0.309	0.616
47	22 × 2	0.43957	0.254	1.781	0.586	0.317	0.617
48	23 × 2	0.45627	3.535	1.862	0.689	0.268	0.687
49	23 × 2	0.43820	0.564	1.864	0.862	0.306	0.620
50	24 × 2	0.44508	0.997	1.783	0.579	0.306	0.636
51	24 × 2	0.42339	3.925	1.816	0.785	0.347	0.558
52	25 × 2	0.44517	1.018	1.879	0.870	0.288	0.649
53	25 × 2	0.44663	1.348	1.881	0.863	0.284	0.655
54	26 × 2	0.45185	2.532	1.790	0.562	0.293	0.660
55	27 × 2	0.43974	0.215	1.856	0.820	0.305	0.624

For the AF interaction we have calculated the slope of the phase boundary critical line, b, which is related to the critical activity, ς_c, at which the lattice gas with infinite nearest-neighbor repulsion undergoes it ordering transition (it corresponds to $T = 0$). In the close vicinity of of the critical point the equation for the phase boundary can be written as

$$\frac{|h|}{|p|} = z - \frac{b}{|p|} + \ldots \tag{39}$$

where $b = (1/2)\ln\varsigma_c$. The endpoints of the boundary line, $\pm h_c$, (the critical value of the magnetic field is determined by the coordination number of lattice $h_c = \pm zp$) correspond to the critical particle surface coverage, θ_c, which determines the range of existence of the ordered $C(2\times 2)$ phase. The values of the critical activities and critical surface coverages had been calculated by Gaunt and Fisher, and Runnels and Coombs [37-39]

$$\varsigma_c = 37962\ldots, \qquad \theta_c = 0.368\ldots \tag{40}$$

Later Baxter, using the method of the corner transfer matrix, obtained these values with very good accuracy [40,41].

Comparing the obtained critical values of the interaction parameters, exponents and thermodynamic functions with the known exact values, one obtains a valuable estimation of the accuracy of the RSRG transformations.

There are two distinctly different types of the blocks. Cell blocks include sites from the both sublattices. Any site of the cell block interacts at least with one another site from the same block. In a sublattice block all sites belong to a single sublattice and interact only with sites that belong to another sublattice blocks. There are no direct interaction between sites inside the block. Some blocks may detyrmined like a mixed type of construction. An inner part of the block forms cell block and outer sites do not interact with this part like in the sublattice blocks. It is an easy task to divide square lattice on blocks. Even linear blocks can be used for RSRG transformations. We have investigated series of 'bricks' with $L = m \times n$, blocks of different star (or snow flake) forms, some pure sublattice blocks.

All RSRG transformations have some general properties. Usually, the RSRG transformations have two fixed points: one for the F interaction $h_c = 0$, $p_c > 0$, and another critical point in the AF half plane of the Hamiltonian parameters $h_c = 0$, $p_c < 0$. Some RSRG transformations have only one fixed point in the F region. In general, the critical values of the interaction parameter, p_c, approach the exact value, p^*, if the number of spins in a block, L, is increased. However, the accuracy of a transformation depends considerably on the symmetry properties of the RSRG block and its composition, i.e. how many sites from different sublattices enter the block. The block symmetry and composition play the decisive roles for the cell RSRG transformations. The most symmetrical blocks show the best critical parameters. This is clearly seen if one compares results obtained for RSRG transformations with blocks of different symmetries but the same size, L (see, for example, series $L = 13$ and 17 in Table 1) and sequences $L = m \times n$. The sublattice, $L \times 2S$, transformations yield rather bad accuracy as compared to the same $L \times 2$ cell transformations. It seems that symmetry does not important for the sublattice RSRG transformations. A good block should have sites from the both sublattice but in some optimum proportion. The main contribution should come from one sublattice and smaller part – from another sublattice. The most accurate results are obtained for the cell RSRG transformation 17×2 (# 38 in Figure 2). The transformation has extremely good accuracy, comparable with the best MC simulations. The block is rather big and has all symmetry elements and composition 5:12. Lowering of the block symmetry and including sites, which do not interact directly with the main body of the block, decrease the critical properties, (compare with another blocks of the same $L = 17$ size).

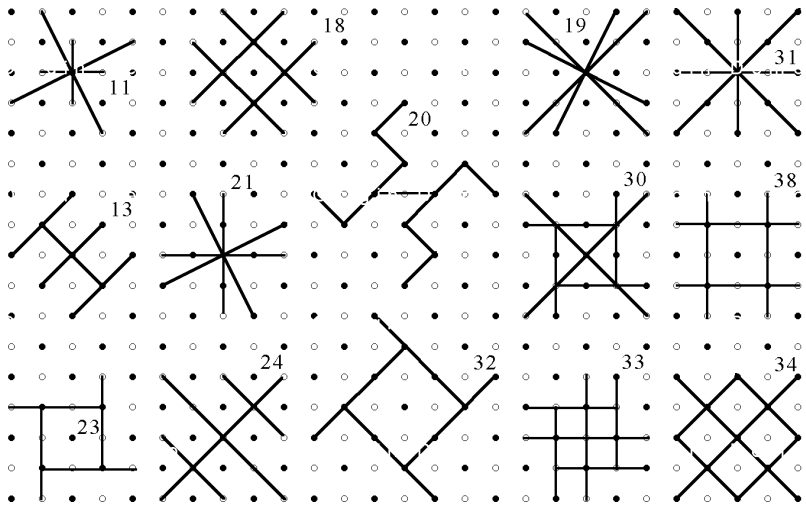

Fig. 2. $C(2\times 2)$ ordered lattice gas phase on a square lattice. There are RSRG blocks of sites shown as polygons and flakes

One should expect, of course, that errors must tend to zero when $L\to\infty$. But even rather small clusters 13×2 have very good characteristics and can be used successfully for investigations of the thermodynamic properties of the Ising spin and lattice gas systems.The most accurate results are obtained for the 17×2 RSRG transformation (# in Figure 3). The transformation has extremely good accuracy, comparable with the best MC simulations.

It should be noted that different critical parameters of the RSRG transformations converge to its exact values with different speeds when block size L is increased. The critical values of the interaction parameter p_c for F and AF interactions have rather good tendencies of convergence to their exact values. The worse converging are quantities related to the second derivative of the free energy over the interaction parameter (temperature): the specific heat and critical exponent y_T. Another critical exponent, y_h, has values rather close to the exact value.

Also, necessary to note that the values of the critical index y_h differ considerably for the F and AF interactions. It follows from the properties of the RSRG transformations. The isothermal susceptibility of the AF Ising model has not power divergence at the critical point. It is related with the quite different behavior of the Ising spin systems with F and AF pair interactions in the external magnetic field. The ferromagnetic susceptibility has strong power divergence. For the Ising ferromagnet strongly correlated fluctuations add, producing divergent susceptibility with large critical index $\gamma = 7/4$. For

repulsive interaction the fluctuations of the sublattice magnetization cancel each other and the residual divergence is much weaker. The temperature series gives logarithmic divergence of the AF susceptibility at the critical point. The isothermal susceptibility of the super-exchange antiferromagnet, derived by Fisher [42], has only vertical tangent at T_c.

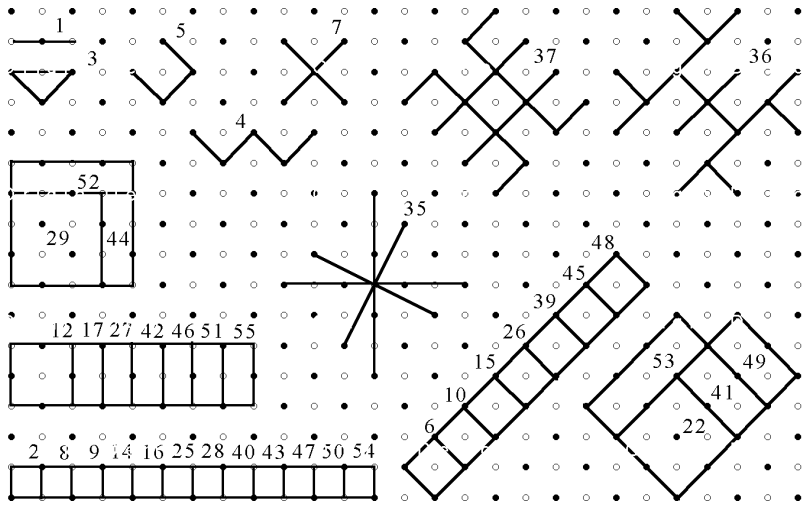

Fig. 3. The RSRG blocks on a square lattice

The logarithmic divergence of the isothermal susceptibility at the AF critical point corresponds to $\gamma_{AF} = 0$. The negative values of the critical index $-1 < \gamma < 0$ give only more or less pronounced sharp peak at the critical point (the dependence is non analytical) of the isothermal susceptibility. In general, the $L \times 2$ RSRG transformations fail to reproduce the weak logarithmic singularities of the specific heat and isothermal susceptibility (at AF critical point). Of course, the above mentioned behavior is rather specific, and it is a hard task for any method to obtain logarithmic singularity.

It is interesting to note that one can apply another "antiferromagnetic majority rule"(AFMR), which can be written in the form of eq. (17). However, spins belonging to different sublattices enter the sum with different signs. The ordinary MR selects configurations depending on their ferromagnetic ordering (total magnetic moment of the block), but the AFMR emphasizes AF ordered configurations (difference of the magnetic moments of sublattices). The results are rather simple: the critical points exchange their places, i.e. $p_F^{(AFMR)} = -p_{AF}^{(MR)}$ and $p_{AF}^{(AFMR)} = -p_F^{(MR)}$.

Tab. 3. Compilation of the AF critical values for the different clusters on a square lattice. $|p_{AF}|$, ε_{AF}, $y_{h,T}$ are the AF critical values of the spin pair interaction parameter, relative error and critical exponents; b and θ_c are the critical slope and coverage at $T = 0$.

#	Cluster	$\lvert p_{AF} \rvert$	ε_{AF} %	y_h	y_T	b	θ_c
	Exact	0.4406868			1.0	0.667	0.368
3	4 × 2	0.42501	3.557	0.753	0.016	0.627	0.357
4	4 × 2S	0.42501	3.557	0.753	0.016	0.627	0.357
5	4 × 2S	0.42501	3.557	0.753	0.016	0.627	0.357
6	5 × 2	0.48223	9.427	0.763	0.346	1.118	0.438
7	5 × 2S	0.36037	18.23	0.613	0.420	0.465	0.311
9	8 × 2	0.43228	1.907	0.693	0.541	1.783	0.473
10	8 × 2	0.31001	29.65	0.694	0.436	0.889	0.392
11	9 × 2	0.39487	10.40	0.728	0.472	0.703	0.372
13	9 × 2S	0.35965	18.39	0.612	0.498	0.553	0.336
15	11 × 2	0.45556	3.374	0.820	0.455	1.069	0.437
16	12 × 2	0.53549	21.51	0.595	0.526	2.173	0.488
18	13 × 2	0.38639	12.32	0.677	0.507	0.636	0.356
19	13 × 2	0.47845	8.570	0.774	0.423	1.165	0.449
20	13 × 2	0.38639	12.32	0.677	0.508	0.636	0.356
21	13 × 2	0.59674	35.41	0.584	0.345	1.963	0.489
22	13 × 2	0.46941	6.517	0.817	0.456	1.167	0.449
23	13 × 2	0.58604	32.98	0.596	0.372	1.963	0.489
24	13 × 2S	0.36744	16.62	0.597	0.523	0.566	0.338
26	14 × 2	0.35774	18.82	0.734	0.480	0.925	0.409
28	16 × 2	0.60510	37.31	0.525	0.484	2.453	0.493
29	16 × 2	0.59796	35.69	0.525	0.468	2.453	0.493
31	17 × 2	0.42406	3.774	0.802	0.506	0.846	0.405
32	17 × 2	0.42406	3.774	0.802	0.506	0.846	0.405
34	17 × 2	0.42406	3.774	0.802	0.506	0.846	0.405
35	17 × 2	0.44475	0.921	0.837	0.498	1.008	0.431
36	17 × 2S	0.36808	16.48	0.590	0.550	0.582	0.343
37	17 × 2	0.38048	13.66	0.652	0.540	0.624	0.354
39	17 × 2	0.46028	4.447	0.791	0.460	1.034	0.434
41	18 × 2	0.39655	10.02	0.704	0.641	1.035	0.429
43	20 × 2	0.65888	49.51	0.481	0.448	2.671	0.495
45	20 × 2	0.39626	10.08	0.691	0.563	0.956	0.418
48	23 × 2	0.47554	7.908	0.733	0.436	1.031	0.434
49	23 × 2	0.45599	3.473	0.850	0.522	1.168	0.451
50	24 × 2	0.70334	59.60	0.450	0.422	2.850	0.497
53	25 × 2	0.46168	4.764	0.844	0.520	1.216	0.456

5. PHASE DIAGRAM

We have calculated the phase diagram for a 2D spin antiferromagnet (and the corresponding lattice gas with repulsive *nn* interaction) using the ordinary MR and AFMR. The diagrams are symmetrical about $h = 0$ and $\theta = 1/2 - ML$. A one half of the critical line is shown in Figure 4. The dependencies of the critical temperature on the magnetic field can be fitted by the following simple expressions

$$T_c(h) = \begin{cases} T_c[1-(h/h_c)^2], & \text{for MR} \\ T_c[1-(h/h_c)^{2,31}]^{0.8}, & \text{for AFMR} \end{cases} \tag{41}$$

Here h_c is the critical magnetic field at zero temperature, $T_c = 0.56818\varphi / k_B$. All RSRG transformations yield the exact value h_c.

Bienenstock and Levis presented a slightly different functional dependence for the critical temperature,

$$T_c(h) = T_c[1-(h/h_c)^2]^{0.87} \tag{42}$$

This expression was obtained using high-temperature expansions of the free energy [43]. The corresponding critical line and is located just between the critical lines given by our MR/AFMR expressions (eq. [41]). It should be noted that the critical line obtained by the AFMR is in very good agreement with an expression supposed by Müller-Hartmann and Zittartz [44],

$$\cosh(h) = \sinh^2(2p) \tag{43}$$

The expression is remarkably simple and reasonably good approximation. If one lets $h, p \to \infty$, keeping activity

$$\varsigma = \exp(8p - 2h) \tag{44}$$

fixed, then the critical value of the activity, obtained from (43) will be $\varsigma_c = 4$ ($T = 0$). It is close to the best numerical estimate $\varsigma_c = 3.7962 \pm 0.0001$ [37]. The dependence is also shown in Figure 4a.

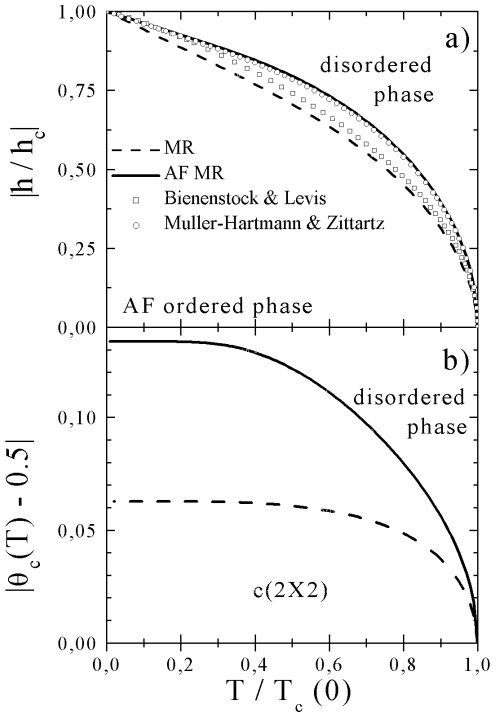

Fig. 4. Phase diagram for (a) square Ising spin system with AF interaction and (b) square lattice gas with lateral repulsion (the values of $|\theta - 0.5|$ are plotted on the Y -axis). The solid lines are obtained with the AF majority rule (AFMR) and the dashed curves represent the ordinary majority rule (MR). The squares are calculated according to Bienenstock and Levis [43]. The circles represent the dependence obtained in Ref. [44]

The deviations between the critical lines obtained by the MR and AFMR RSRG approaches are relatively small in the $h - T$ plane, but much stronger deviations arise when we consider the phase boundary between ordered and disordered lattice-gas phases in the $\theta - T$ plane (see Figure 4b). The ordinary MR approach yields a very narrow region near half coverage for the existence of the $C(2\times 2)$ ordered phase, $0.437 \le \theta \le 0.563$ (dotted line in Figure 4b). The AFMR approach gives a significantly wider stability range of this phase, $0.366 \le \theta \le 0.634$ (solid line). This range coincides rather well with the results obtained by Runnels and Combs [38], $0.371 \le \theta \le 0.629$.

6. ADSORPTION ISOTHERMS AND CORRELATION FUNCTIONS

Using the most accurate 17×2 cell RSRG transformation we have calculated temperature and coverage dependencies of various thermodynamic quantities for an interacting lattice gas on a square lattice. In this Section we consider the first derivatives of the free energy over its independent variables, namely, surface coverage as function of the chemical potential and correlation function P_{00}.

For the calculations of adsorption isotherms, $\theta(\mu)$, by the RSRG method we use the following expression

$$\theta(\mu)=\frac{\partial F}{\partial \mu}\equiv\frac{1}{2}\left[1+\left(\frac{\partial F}{\partial h}\right)\right] \tag{45}$$

Adsorption isotherms are plotted in Figures 5 and 6. The coincidence between RSRG and MC data is very good for the whole range of temperatures and surface coverage studied. At high temperatures the dependencies are close to the Langmuir case $(\varphi=0)$

$$\theta(\mu)=\exp(\mu+\varepsilon)[1+\exp(\mu+\varepsilon)]^{-1} \tag{46}$$

As the temperature decreases, the behavior of the dependencies depends on the sign of the pair interaction. For repulsive interaction between particles the slope of the curves at $\theta=1/2-ML$ decreases and at the critical temperature the dependencies became flat. The peculiarity corresponds to the second order phase transition. The disordered system of particles becomes ordered in the close vicinity of the half monolayer coverage. The peculiarity turns into a broad horizontal plateau as temperature decreases well below T_c. The plateau represents the formation of the ordered $C(2\times 2)$ phase, when the translation-invariance symmetry is spontaneously broken: the whole lattice is subdivided into sublattices with different occupancies. At zero temperature the $C(2\times 2)$ phase exists in the region $[\theta_c,1-\theta_c]$. The values of the critical coverage depends on the lattice symmetry. The values of θ_c for different RSRG transformations are compiled in Table 3. In order to show clearly the critical behavior of the adsorption isotherms we have built a 3D chart, shown in Figure 5. The total number of the MC points exceeds 400.

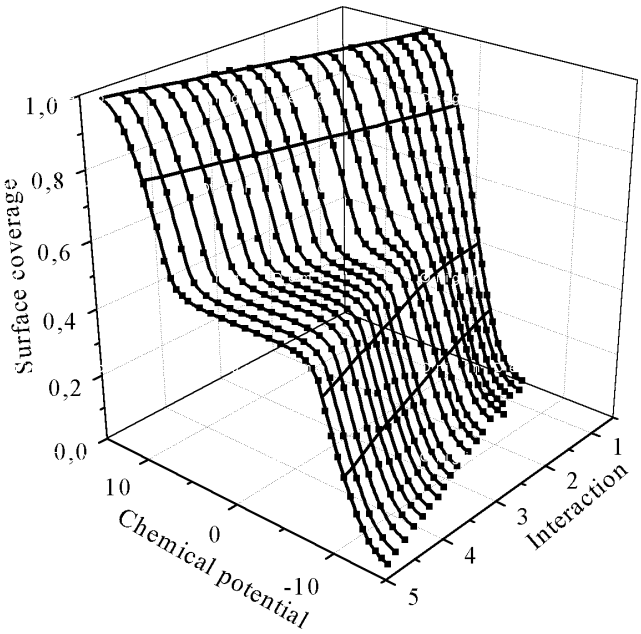

Fig. 5. 3D chart of adsorption isotherms (θ vs. $(\mu+\varepsilon-2\varphi)/2k_BT$ and $|\varphi|/k_BT$). Repulsive lateral interaction. Solid lines and symbols are the RSRG and MC data, respectively

For attractive interaction between the particles the decreasing of the temperature causes increase of the slope at $\theta = 1/2 - ML$. The dependence becomes steeper and steeper and at the critical temperature the second derivative of the free energy over the chemical potential diverges. The further decrease of the temperature leads to the discontinuous behavior of the absorption isotherms as shown in Figure 6. At some value of the chemical potential μ_c, corresponding to $h = 0$, the coverage jumps between $\theta(\mu_c - 0)$ and $\theta(\mu_c + 0)$. It is the phase transition of the first order. In the grand canonical ensemble description in the region $\theta(-0) < \theta < \theta(+0)$ is impossible. At the critical value of the chemical potential surface coverage is a non analytical function of μ. Kadanoff marked this region ($h = 0$, $T \le T_c$) as "no stable thermodynamic states" [27]. The system becomes inhomogeneous. There are islands of a dense, $\theta \approx 1$, phase randomly immersed in a rarefied background with coverage $\theta \to 0$. There is continuous exchange by particles between these phases, some islands disappear, some grow. The kinetic behavior of the system is rather complex.

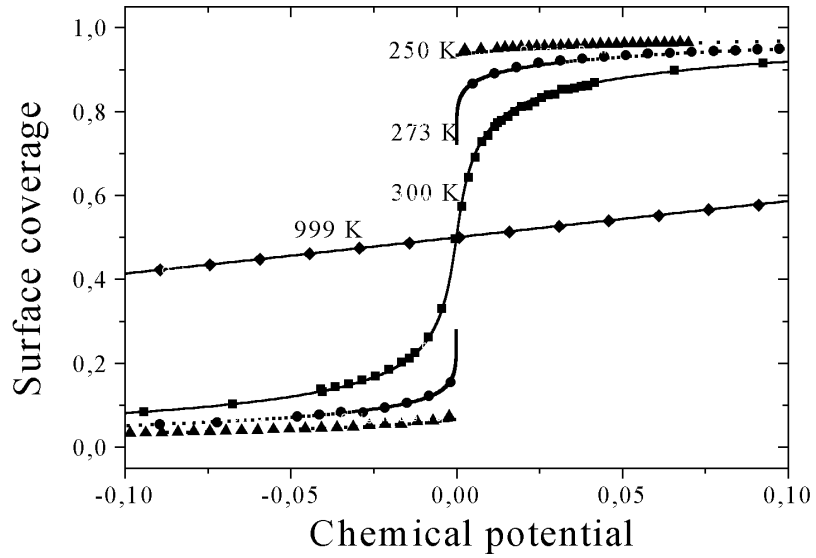

Fig. 6. Adsorption isotherms (θ vs. $(\mu+\varepsilon-2\varphi)/2k_BT$) for different tempera–tures. Attractive lateral interaction. The value of the interaction parameter φ is equal to 4 kJ/mol. Solid lines and symbols are the RSRG and MC data, respectively

The exact temperature dependence of the critical endpoints of the adsorption isotherms $\theta(\mu\pm 0)$ proportional to the spontaneous magnetization at zero external magnetic field, $m=\langle s_i\rangle$. The latter was obtained by Yang [45]

$$\left|2\theta(\pm 0)-1\right| \equiv m = \left[1-\sinh^4(2\varphi)\right]^{1/8} \tag{47}$$

The dependence is plotted in Figure 7. The corresponding RSRG data are shown as symbols. The coincidence with the exact curve is rather good.

We have also investigated the coverage dependencies of the correlation function P_{00}, which is needed to calculate the chemical diffusion coefficient D_c. This quantity is the probability to find two holes on the nn sites. It is proportional to the first derivative of the first energy over the interaction parameter φ. Thus it does not show singular dependence at the critical points. For repulsive and attractive interactions as well, P_{00} is a smooth function of the surface coverage shown in Figures 8 and 9. At high temperatures P_{00} is close to the mean-field result

$$P_{00} = (1-\theta)^2$$

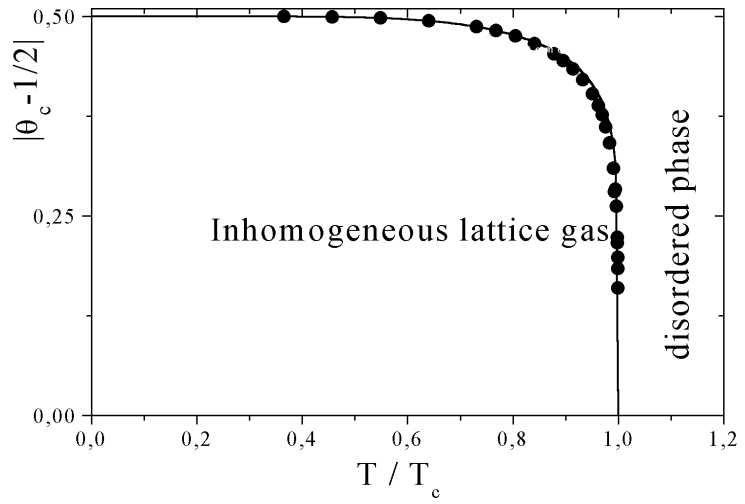

Fig. 7. The critical line of the first order phase transition $|(2\theta(\pm 0)-1|$ vs. T/T_c) in the square lattice gas obtained in Ref. [45]. Symbols are the RSRG data

For repulsive interaction and low temperatures P_{00} decreases almost linearly to very small values at half coverage, i.e.

$$P_{00} \approx 1-2\theta \text{ for } 0<\theta<1/2 \tag{48}$$

This result is clearly due to the fact that in this range of coverage particles are able to avoid each other and, therefore, every particle adsorbing on the surface destroys 4 two-hole configurations. Thus, the probability to find such configurations can be expressed as $1-4\times$ (number of particles)/(number of bonds) = $1-2\theta$.

In contrast, attractive interactions increases the probability of finding pairs of *nn* particles and, therefore, the number of hole pairs increases also. At low temperatures the correlation function P_{00} approaches line $1-\theta$. Again, the coincidence between RSRG (lines) and MC data (symbols) is rather good throughout the whole ranges of temperatures and coverage.

7. ISOTHERMAL SUSCEPTIBILITY AND SPECIFIC HEAT

The quantities, being the most sensitive to phase transitions, are the second derivatives of the free energy, F, over the chemical potential – isothermal susceptibility, χ_T, and temperature – specific heat, C_h. The second derivative of the free energy over the chemical potential is equal to the mean square surface coverage fluctuations

$$\chi_T = \frac{\partial^2 F}{\partial \mu^2} \tag{49}$$

This quantity is proportional to the mean square fluctuations of the magnetization of the spin system. The coverage dependencies of the isothermal susceptibility are plotted in Figures 10 and 11 for the repulsive and attractive pair lateral interaction, respectively.

At high temperatures (Langmuir case) the mean square surface coverage fluctuations are described by the following expression

$$\chi_T = \theta(1-\theta) \tag{50}$$

As the temperature decreases the behavior of the isothermal susceptibility is quite different for the different signs of the lateral interaction. In case of repulsive interactions the coverage dependencies, $\chi_T(\theta)$, have a deep and narrow minimum at half coverage and low temperatures but remains analytical function of μ. The minimum corresponds to an almost perfectly ordered $C(2\times 2)$ structure. Then any coverage disturbance (i.e., the displacement of a particle from its `right' position in the filled sublattice to any site of the empty sublattice) increases considerably the energy of the system and is thermodynamically unfavorable. Thus, mean square coverage fluctuations are strongly suppressed. For any coverage $\theta \neq 1/2 - ML$, there are fluctuations of the non-stoichiometric nature that do not require additional energy for their existence. These fluctuations cannot by removed from the system by particle jumps. Therefore, χ_T increases when θ deviates from half coverage.

It is also interesting to note that at low temperatures the fluctuations have two tiny maxima at the critical points (see the arrows in Figure 10). The coverage dependencies are non-analytical in these points of the second order phase transition.

There is a good coincidence between the RSRG and MC data in the whole range of coverage. However, deviations are seen in the vicinities of the critical points.

For attractive interactions the mean square surface coverage fluctuations are also close to the Langmuir case eq. (50) at hight temperature. Upon decreasing the temperature the coverage fluctuations exhibit a sharp maximum at half coverage, growing to infinity as $T \to T_c$. Any surface coverage disturbance relaxes slower and slower as the lateral interaction between particles approaches to its critical value. The system becomes unstable in the critical point and the fluctuations are strongly divergent.

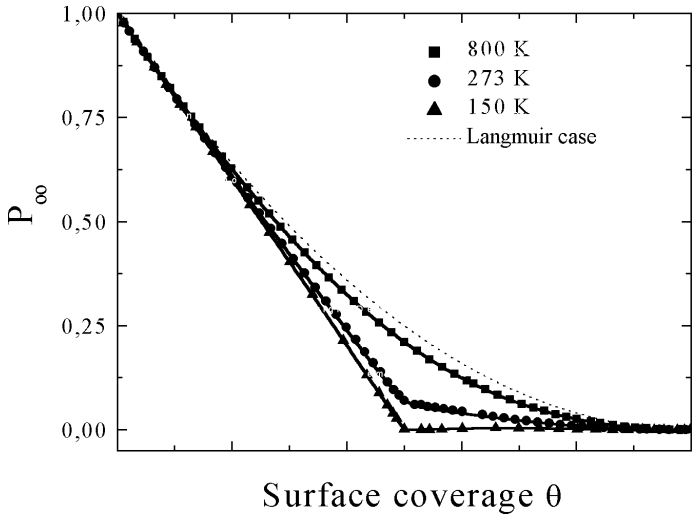

Fig. 8. Coverage dependence of the pair correlation function P_{00} for different temperatures as indicated. Repulsive interaction. The dotted line represents the mean-field result $P_{00} \equiv (1-\theta)^2$. Solid lines and symbols are the RSRG and MC data, respectively

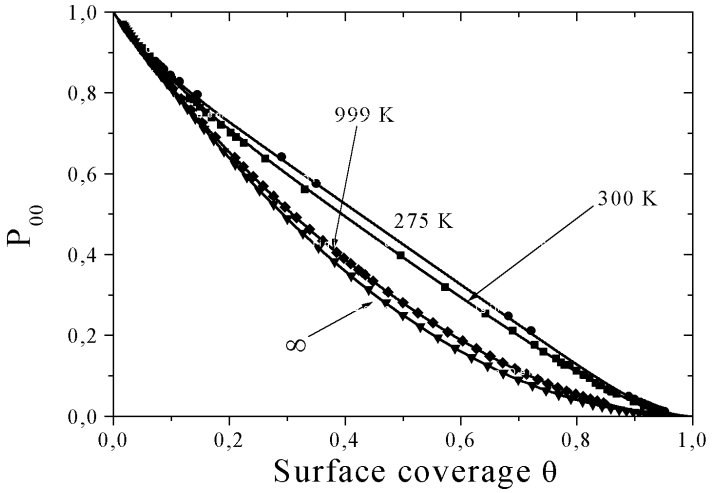

Fig. 9. Coverage dependence of the pair correlation function P_{00} for different temperatures as indicated. Lateral attraction. The dotted lines represents the mean-field result $P_{00} \equiv (1-\theta)^2$. Solid lines and symbols are the RSRG and MC data, respectively

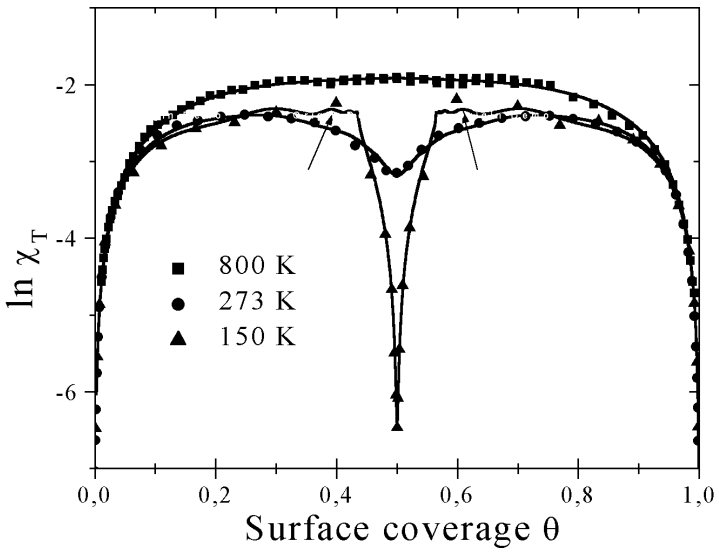

Fig. 10. Coverage dependence of the mean square coverage fluctuations ($\ln \chi_T$ vs. θ) for different temperatures as indicated ($k_B T / |\varphi|$). Repulsive interaction, $|\varphi|$=4 kJ/mol. Solid lines and symbols are the RSRG and MC data, respectively

The critical singular behavior is well described by the following scaling law

$$\chi_T \propto (T - T_c)^{\gamma} \tag{51}$$

with

$$\gamma = \frac{2y_h - 1}{y_T} \approx 2.05 \tag{52}$$

The dependence is plotted in Figure12. The exact value of the critical exponent γ for the Ising spin model is well known $\gamma = 7/4$. The best fit line of the RSRG data has the slope 2.05, which is in a rather good agreement with the value of the critical exponent. Even for the second derivative of the free energy over chemical potential, having rather sharp coverage and temperature dependencies, we have obtained a good coincidence between the RSRG and MC data in the whole coverage region for different temperatures, excluding only the close vicinity of the critical points.

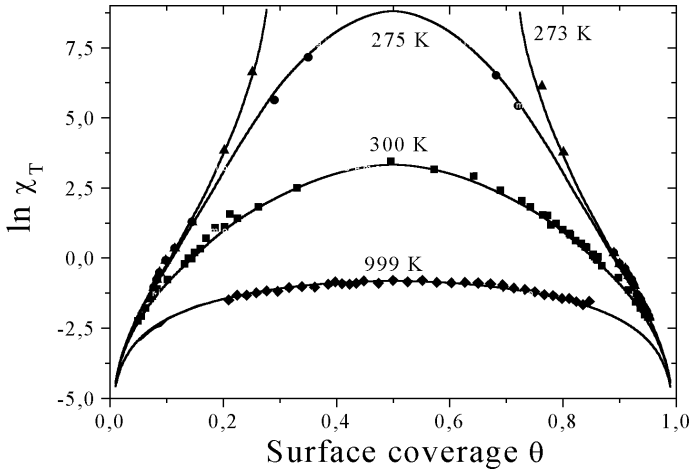

Fig. 11. Coverage dependence of the mean square coverage fluctuations ($\ln \chi_T / 4$ vs θ) for different temperatures as indicated. Attractive interaction, φ =4 kJ/mol. Solid lines and symbols are the RSRG and MC data, respectively

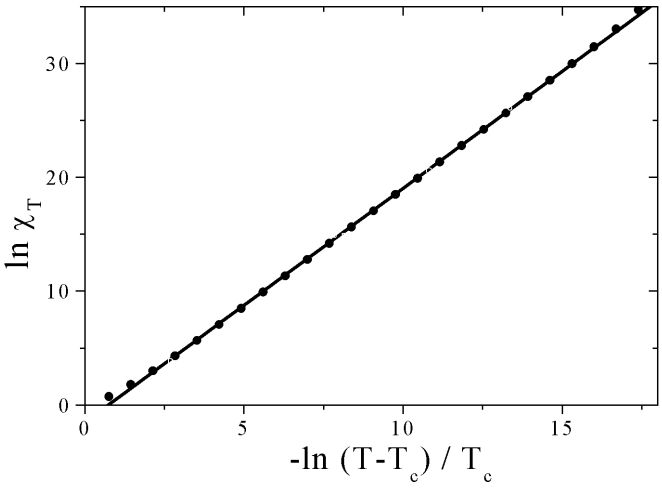

Fig. 12. The critical growth of the mean square coverage fluctuations ($\ln \chi_T$ vs. $\ln(T/T_c - 1)$). Symbols are the RSRG data, solid line is the best fit. Lateral attraction between particles

We have calculated also the second derivative of the free energy F over the interaction parameter p, which is used to calculate the specific heat C_h

$$C_h \equiv T\left(\frac{\partial^2 F}{\partial T^2}\right)_V = \frac{1}{T}\frac{\partial}{\partial p}\left(p^2 \frac{\partial F}{\partial p}\right)_h \tag{53}$$

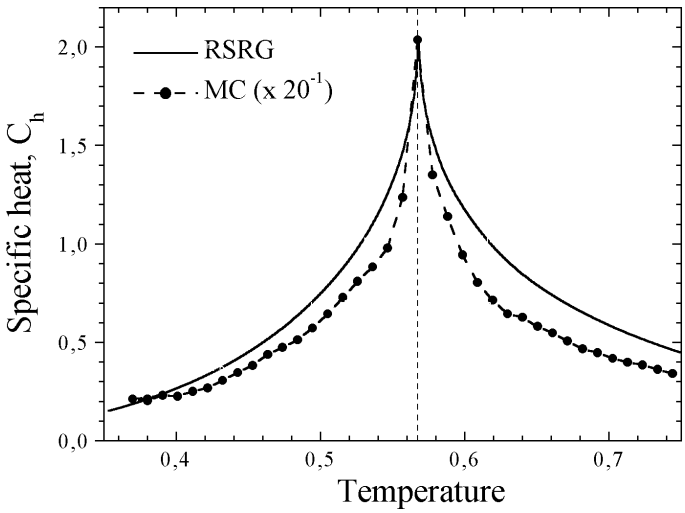

Fig. 13. The temperature dependence of the singular part of the specific heat C_h. Lateral attraction, φ = 4 kJ/mol. Dashed line corresponds to the exact value of the critical temperature. Solid lines and symbols are the RSRG and MC data, respectively. MC data are decreased by 20

The temperature dependence of the singular part of the specific heat, C_h, is shown in Figure 13. The MC data differ considerably from the RSRG results. We have divided the MC data by 20 in order to show the coincidence of the critical temperatures obtained by the different methods. It should be noted, that the height of the peak, obtained by the RSRG method, depends strongly on the the critical exponent eigenvalue y_T. The scaling behavior of the singular part is given by:

$$C_h \approx -(T - T_c)^{-\alpha}, \text{ where } \alpha = 2(y_T - 1)/y_T \tag{54}$$

If the value of the critical exponent y_T is equal to 1, which corresponds to $\alpha = 0$, the second derivative of the free energy over pair interaction parameter

becomes divergent as $\ln(T/T_c - 1)$. All RSRG transformations have critical exponent $y_T < 1$. The bigger is the value of the critical exponent y_T, the higher is the peak of the specific heat C_h. For $y_T < 2/3$ the peak does not appear at all and dependence will be a smooth curve without peculiarities.

8. DIFFUSION COEFFICIENTS

In this section we consider the coverage and temperature dependencies of diffusion coefficients obtained by the RSRG and MC methods. We have calculated the tracer, jump and chemical diffusion coefficient for different temperatures in the whole range of the surface coverage.

The coverage dependencies of the tracer diffusion coefficient are plotted as 3D chart in Figure 14. At $\theta = 0.5$, $D_t(\theta)$ presents a very deep and narrow minimum, which becomes more pronounced as the temperature is decreased. It is the effect of ordering in the system of particles. Repulsion between particles causes a second order phase transition from a disordered structure (at high temperatures) to the ordered $C(2\times 2)$ arrangement. The ordered phase exists in a coverage region centered at half monolayer ($\theta = 0.5$). In this phase, empty and filled lattice sites alternate each other. The influence of repulsive lateral interaction drastically changes the smooth coverage dependence of D_t at high temperatures. The presence of a minimum in the surface coverage dependence of D_t can be explained if one use the approximate expression for the tracer diffusion coefficient [46]

$$D_t = fV\langle P_{ij}\rangle \tag{55}$$

Here f is the tracer correlation factor, V is the vacancy availability factor and $\langle P_{ij}\rangle$ is the average jump probability. The minimum of D_t at half coverage basically reflects minima of the average jump probability $\langle P_{ij}\rangle$ and the correlation factor f.

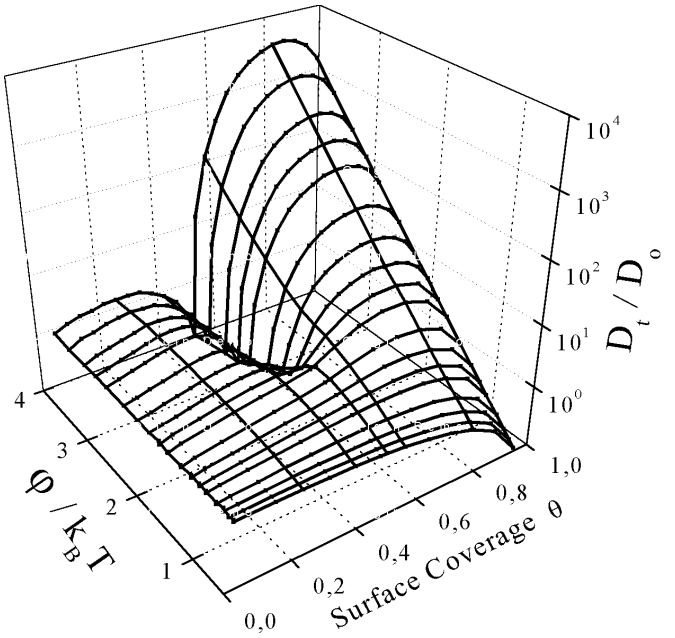

Fig. 14. 3D chart of the dependencies $\ln D_t / D_0$ vs. θ and $|\varphi| / k_B T$. Lateral repulsion, $|\varphi| = 4$ kJ/mol

We present the coverage dependencies of the jump diffusion coefficient, D_J, in Figure 15. The characteristic shapes of the tracer and jump diffusion coefficients are almost identical indicating that D_t and D_J behave quite similar despite their fundamental different meanings of the coefficients. As already mentioned, the tracer diffusion coefficient describes the motion of tagged particles on the surface while the jump diffusion coefficient represents the mobility of the center of mass of the system. Both quantities are numerically equal only if the cross-correlation terms are absent. The curves are straight lines only for small and high surface coverages. The lateral interaction decreases the activation energy of diffusion. It is seen clearly for small coverage and for coverage close to the monolayer but at the intermediate coverage another factor – the availability of the empty sites around the jumping particle – plays the decisive role. At the half coverage and low temperatures the particle almost immobile due to the strictly ordered $C(2\times 2)$ phase. The jump diffusion coefficient has deep minimum at this coverage (like the tracer diffusion coefficient) due to the ordering in the particle system.

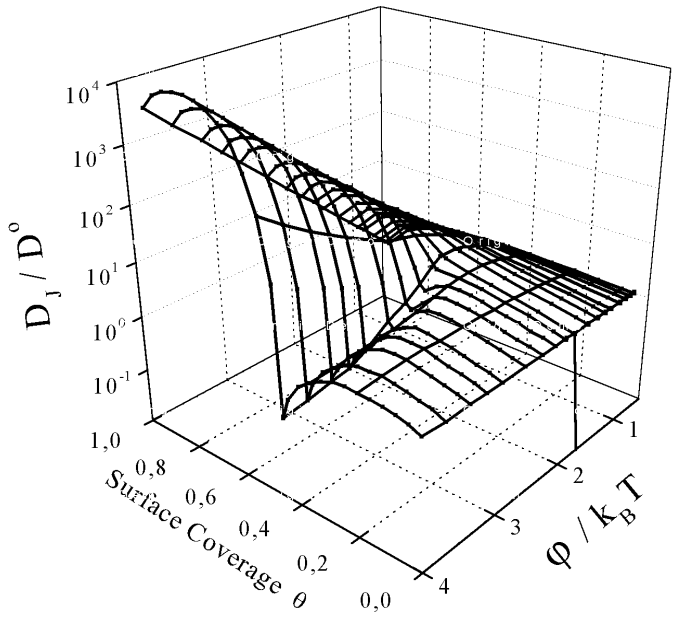

Fig. 15. 3D chart of the dependencies $\ln D_t / D_0$ vs. θ and $|\varphi| / k_B T$. Lateral repulsion, $|\varphi|$=4 kJ/mol

The coverage dependencies of the chemical diffusion coefficient are plotted in Figure 16. In the limits of $\theta \to 0{,}1$, a jumping particle has none or three nearest neighbors, respectively. Therefore, the limiting values of the chemical diffusion coefficient, D_c are equal to

$$\begin{aligned} &\lim_{\theta \to 0} D = D_0 \\ &\lim_{\theta \to 1} D = D_0 \exp(3\varphi / k_B T) \end{aligned} \tag{56}$$

For small surface coverage $\theta 1 - ML$, in the disordered lattice gas phase, $\ln D_c$ changes almost linearly with θ. This behavior reflects the increase of the mean number of *nn*s for any jumping particle. It is interesting to note that qualitatively same behavior can be seen at large coverage slightly below monolayer coverage, where $\ln D_c$ decreases almost linearly with θ. In this case the relaxation of coverage fluctuations proceeds via the diffusion of holes, whose density is given by $1 - \theta$. Therefore, the linear decrease of $\ln D_c$ with θ is comprehensible. It is probably important to note, that due to the particle-hole

symmetry of the lattice gas Hamiltonian, the repulsive interaction energy for holes is also given by φ.

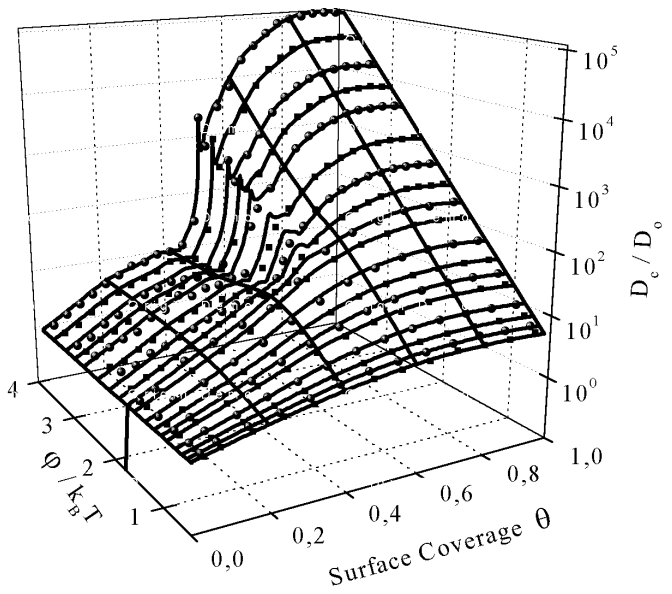

Fig. 16. 3D chart of the dependencies $\ln D_t / D_0$ vs. θ and $|\varphi| / k_B T$. Lateral repulsion, $|\varphi|$=4 kJ/mol

There are two tiny minima on the coverage dependencies $D_c(\theta)$ at the critical points corresponding to the second order phase transition between the dilute lattice gas $\leftrightarrow C(2\times 2)$ ordered phase $\leftrightarrow$ dense lattice fluid. Upon approaching the critical points, the coverage fluctuations grow and cause the reduction of the diffusion coefficient. The minima of the diffusion coefficient correspond to the maxima of the mean square surface coverage fluctuations, see Figure 10.

Attraction between particles cause a first order phase transition below a critical temperature T_c. As the temperature decreases, lateral interaction more and more inhibits the relaxation of coverage fluctuations. At the critical temperature the system becomes unstable and its properties drastically change. The homogeneous in average system decomposes into domains of low and high local surface coverage.

Attractive interaction between nns reduces mobility of particles. But the tracer and jump diffusion coefficients do not show any critical peculiarities and are smooth functions of the surface coverage. The chemical diffusion coefficient decreases relative to the Langmuir case: $D_c(\theta) < D_0$ for all surface

coverage and $\ln D_c$ exhib its a broad minimum at coverage around $\theta \approx 0.5$ (see Figure 17). In the gas phase the $\ln D_c / D_0$ decreases almost linearly with the coverage θ, as the mean number of nn s for any jumping particles is increasing. Qualitatively the same behavior one can see at coverage slightly less then 1-ML. The coincidence between the RSRG and MC data is good only for high temperatures. At low temperatures the mobility of the particles decreases substantially. To obtain the reliable MC data necessary to carry out very long simulations.

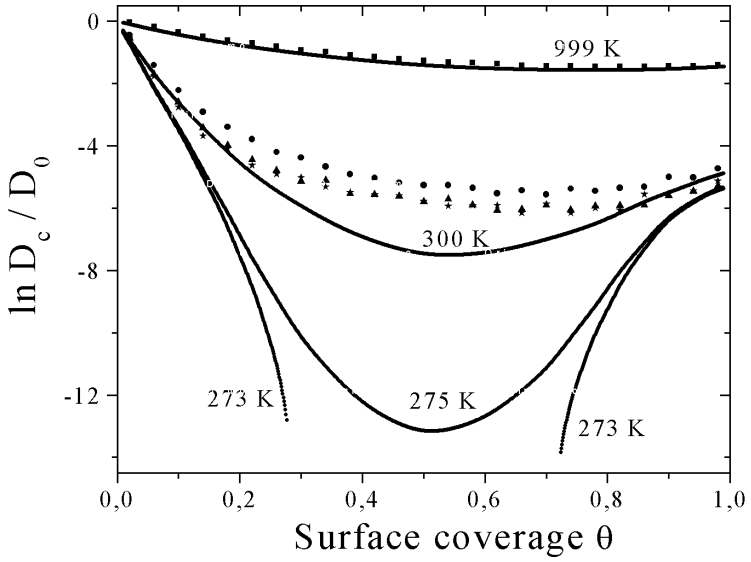

Fig. 17. Coverage dependencies of the chemical diffusion coefficient $\ln D_t / D_0$ vs. θ in case of attractive interaction. Solid lines are obtained by the RSRG approach, symbols denote MC data

When approaching critical point the mean square coverage fluctuations diverge, $\chi_T \to \infty$, and cause the critical slowdown of the chemical diffusion coefficient at the half monolayer coverage. The behavior of the chemical diffusion coefficient in the vicinity of the critical point is described by the critical exponent $-\gamma$, i.e.

$$D_c \approx (T - T_c)^{\gamma} \tag{57}$$

The critical slowdown of the chemical diffusion coefficient is plotted in Figure 18. At the critical point the diffusion coefficient is equal to zero.

Diffusion relaxation of the surface coverage disturbances is switched off and the system becomes inhomogeneous. If $T < T_c$ the region of the lattice gas inhomogeneity widened symmetrically around $\theta = 0.5$ in accordance with the expression eq. (41).

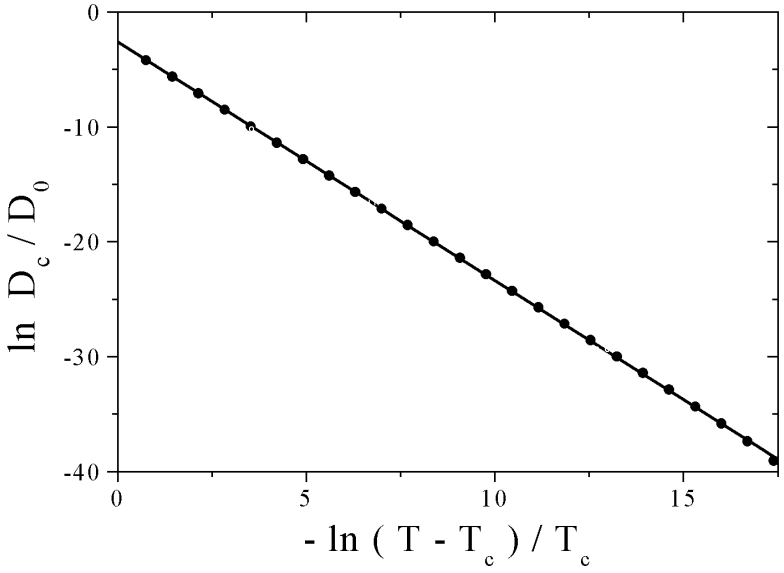

Fig. 18. The critical slowdown of the chemical diffusion coefficient $\ln D_c / D_0$ vs. $\ln(T/T_c - 1)$ at the half monolayer coverage. Symbols are the RSRG data, solid line is the best fit. Lateral attraction between particles

It should be noted that the chemical diffusion coefficient behavior in the critical region is determined completely by the critical divergence of the surface coverage fluctuations and does not depend on the model of jumps used for derivation of the expression, eq. (11). This conclusion is based on the fact, that all other quantities entering eq. (11) vary slowly in the critical region.

To finish with the surface diffusion coefficients we discuss shortly also their temperature dependencies plotted in Figures 19–21. A first inspection already shows that the influence of repulsive lateral interactions drastically changes the smooth dependence of D_t at high temperatures (see Figure 19). For surface coverages far apart from $\theta = 0.5$, Arrhenius (linear)behavior is seen for a wide range of temperatures, i.e. $\log D_t \propto (k_B T)^{-1}$. At half monolayer the dependencies have deep minimum. and temperature dependency $\log D_t(\theta = 0.5)$ vs $1/T$ exhibits a maximum close to T_c. The increase of the activation energy E_t seen above $\geq T_c$ represent the repulsive ad-ad interactions, while positive

activation energies below $\leq T_c$ are due to the $C(2\times 2)$ ordering of the lattice gas. In order to explain this observation we note that the mean number of nearest neighbors decreases strongly in the ordered $C(2\times 2)$ phase and, as a consequence, the slope of the curve decreases as well.

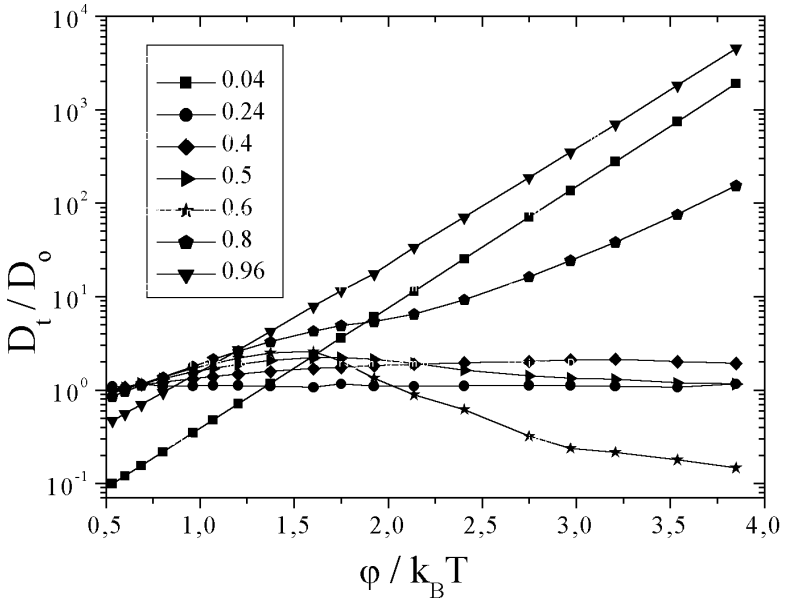

Fig. 19. The temperature dependencies of the normalized tracer diffusion coefficient $\ln D_t / D_0$ for some representative values of θ. Lateral repulsion between adsorbed particles, $|\varphi|$ = 4 kJ/mol

In Figure 20, we present the temperature dependencies of the jump diffusion coefficient D_J. The characteristic shapes of Figures 19 and 20 are almost identical indicating that D_t and D_J behave quite similar despite their fundamental different meanings. As already mentioned, the tracer diffusion coefficient describes the motion of tagged particles on the surface while the jump diffusion coefficient represents the mobility of the system center of mass. Both quantities are numerically equal only if there are no velocity-velocity cross correlation terms [3].

The temperature dependencies of the chemical diffusion coefficient are plotted in Figure 21. They are smooth functions. Only weak departures from linearity are visible at the intermediate coverages. At small coverages the activation energy is equal to the potential depth ε. Close to the monolayer activation energy grows due to the lateral repulsion between the particles.

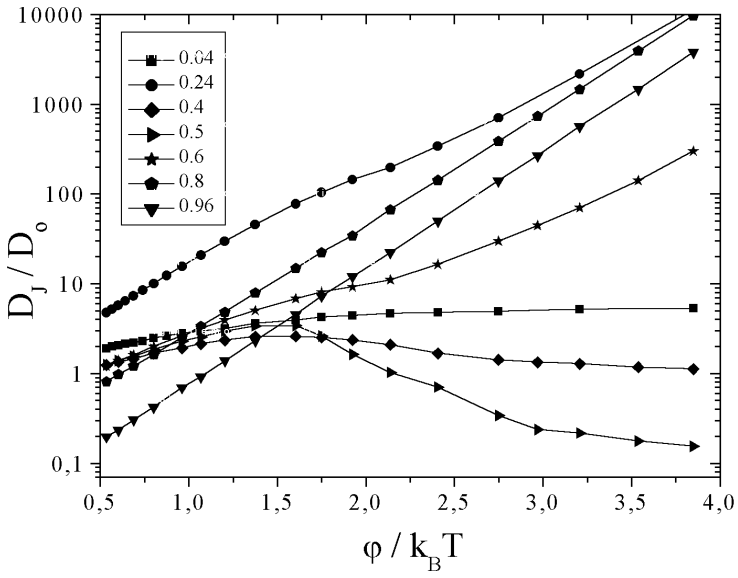

Fig. 20. As Figure 19, for the jump diffusion coefficient, D_c / D_0

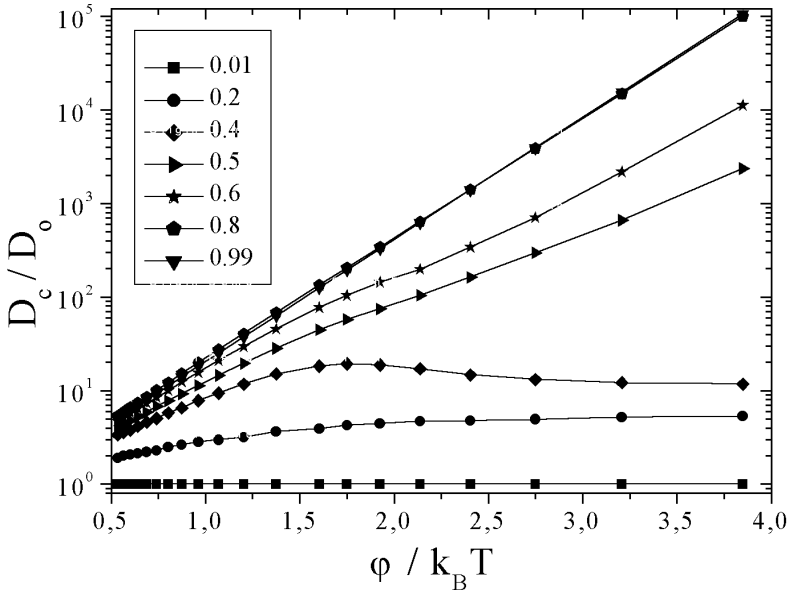

Fig. 21. As Figure 19, for the chemical diffusion coefficient, D_c / D_0

9. SUMMARY

We present results of investigations of the surface diffusion of adsorbed particles on the square lattice with account of the strong lateral interaction between the particles using the RSRG and MC methods.

A large number of RSRG transformations with blocks of different size and symmetry have been investigated. It is shown that the precision of the RSRG method strongly depends not only on the size of the blocks but also on their symmetry and composition. In general, the accuracy of the RSRG method increases with the number of sites in the block. But choosing the rather small blocks with optimal symmetry and composition it is possible to reach very good results. The most accurate data have been obtained for the relatively small clusters 34 sites. The minimal relative error in determining the critical values of the pairwise interaction parameter is equal to 0.13 %. Using the RSRG method we explored the phase diagram of a square antiferromagnet in an external magnetic field and the corresponding phase diagram of a lattice gas on a square lattice with repulsive nn interaction. The critical temperature, the critical magnetic field and the critical surface coverage at $T = 0$ coincide rather well with the known values for these parameters.

We have calculated the coverage and temperature dependencies of the tracer, jump and chemical diffusion coefficients, the mean square surface coverage fluctuations and the pair correlation function of nearest neighbor particles. We have obtained also the adsorption isotherms for different temperatures above and below the critical point. We have analyzed the critical growth of the particle surface coverage fluctuations in the vicinity of the critical point and the corresponding critical slowdown of the chemical diffusion coefficient. The phase transitions and processes of ordering in two-dimensional systems cause extremely sharp behavior of the chemical diffusion coefficient and coverage fluctuations. Critical fluctuations are rather strong and bring valuable information about the processes which take place on the crystal surfaces.

Using a fully parallelized algorithm in conjunction with Cray T3E (LC768-128) parallel computer operated by the Max-Planck community in Garching/Germany, we have calculated thermodynamic properties and tracer, jump and chemical diffusion coefficients in the wide temperature region and full range of the surface coverage by using the extensive MC simulations.

The RSRG data are compared with the well-known exact expressions and MC results. The coincidence between the exact and RSRG data is rather good. Also the agreement between the results obtained by the quite different RSRG and MC methods is surprisingly good. Therefore, we can conclude that the RSRG method appears to be a rather reliable method which can be used for investigations of the thermodynamic and kinetic properties of many strongly interacting adsorbate systems.

Acknowledgements. This work has been supported by the grant LN00A015 of the MŠMT ČR.

REFERENCES

[1] *Equilibria and dynamics of gas adsorption on heterogeneous solid surfaces*, Eds. W. Rudzinski, W. Steele and G. Zgrablich, Elsevier, Amsterdam, 1996; Zhdanov V.P., *Elementary Physicochemical Processes on Solid Surfaces*, Plenum, Newy York (1991); Baxter R.J., *Exactly Solved Models in Statistical Mechanics*, Academic Press, London, 1982; Rudzinski W. and Everett D., *Adsorption of Gases on Heterogeneous Surfaces*, Academic Press, New York, 1992.

[2] Kehr K. and Binder K., *in Applications of the Monte Carlo Method in Statistical Physics*, Vol. 36 of *Topics in Current Physics*, 2 ed., Ed. by K. Binder (Springer-Verlag, Berlin, 1987), p. 181; Binder K., in *Phase Transitions and Critical Phenomena*, edited by C. Domb and J.L. Lebowitz (Academic Press, New York, 1983), Vol. IIX, p.1; K. Binder, in *Finite Size Scaling and Numerical Simulation of Statistical Systems*, edited by V. Privman (World Scientific, Singapore, 1990); Binder K., *Rep. Prog. in Phys*. 60, 488 (1997). Landau D.P., in *Monte Carlo Methods in Statistical Physics*, edited by K. Binder (Springer-Verlag, Berlin, 1979).

[3] Gomer, R., *Rep. Prog. Phys.*, 53, 917, (1990).

[4] Ala-Nissila T., Ferrando R., Ying, S.C., *Advances in Physics* 51, 949 (2002).

[5] Tarasenko A.A. and Chumak A.A., *Fiz. Tverd. Tela (Leningrad)* 24, 2972 (1982), [*Sov. Phys. Solid State* 24, 1683 (1982)], Chumak, A.A. and Tarasenko, A.A., *Surf. Sci.*, 91, 694, (1980).

[6] Ala-Nissila T. and Ying S.C., *Phys. Rev.* B42, 10264 (1990).

[7] Danani A., Ferrando R., Scalas E. Torri M., *Int. Jour. of Mod. Phys.* B11, 2217,(1997).

[8] Gortel Z.W., Zoluska-Kotur M.A., Turski L.A., *Phys. Rev.* B52, 16916 (1995).

[9] Tarasenko A.A. and Chumak A.A., *Fiz. Tverd. Tela (Leningrad)* 22, 2939 (1980), [*Sov. Phys. Solid State* 22, 1716 (1980)].

[10] Tarasenko A.A. and Chumak A.A., *Poverkhnost' Fiz.Khim. Mekh.* 11, 98 (1989), (in Russian).

[11] Tarasenko A.A., Jastrabik L., Uebing C, *Phys. Rev.* B57, 10166 (1998).

[12] Tarasenko A.A., Jastrabik L., Nieto F., Uebing C., *Phys. Rev.* B59, 8252 (1999).

[13] Tarasenko A.A., Nieto F., Uebing C., *Physical Chemistry Chemical Physics (PCCP)* 1, 3437 (1999).

[14] Tarasenko A.A., Nieto F., Jastrabik L., Uebing C., *Phys. Rev.* B64, 075413 (2001).

[15] Kehr K.W., Kutner R., Binder K., *Phys. Rev.* B23 4931 (1981); B26 2967 (1982).

[16] Haus J.W. and Kehr K.W., *Phys. Rep.* 150, 263 (1987).

[17] Ala-Nissila T., Han W.K., Ying S.C., *Phys. Rev. Lett.* 68, 1866 (1992).

[18] Vattulainen I., Merikoski J., Ala-Nissila T., Ying S.C., *Phys. Rev. Lett.* 79, 257 (1997).

[19] Onsager L.., *Phys. Rev.* 65, 117 (1944).

[20] Wilson K.G., *Phys. Rev.* B4, 3174 (1971).

[21] Wilson K.G., *Phys. Rev.* B4, 3184 (1971).

[22] Niemeijer, Th. and van Leeuwen, J. M. J., *Phys. Rev. Lett.*, 31, 1412 (1973).

[23] Niemeijer, Th. and van Leeuwen, J. M. J., *Physika*, 71, 17 (1974).

[24] Nauenberg, M. and Nienhuis, B., *Phys. Rev. Lett.* 33, 1598 (1974).

[25] Nauenberg, M. and Nienhuis, B., *Phys. Rev. Lett.* 35, 477 (1975).

[26] Kadanoff L.P., *Physics* 2, 263 (1966).

[27] Kadanoff L.P. et al, *Rev. Mod. Phys.* 39, 395 (1967).

[28] Sabbaswamy K.R. and Mahan G.D., *Phys. Rev. Lett.* 37, 642 (1976).

[29] Mahan G.D. and Claro F.H., *Phys. Rev.* B16, 1168 (1977).

[30] Schick M., Walker J.S. Wortis M., *Phys. Lett.* A58, 479 (1976).
[31] Schick, M., Walker J.S., Wortis M., *Phys. Rev.* B16, 2205 (1977).
[32] Niemeijer, Th.and van Leeuwen, J.M.J., in *Phase Transitions and Critical Phenomena*, Eds.: C. Domb, M.S. Green, vol. VI, chap. 7, Academic Press, New York, 1976.
[33] Nienhuis B. and Nauenberg M., *Phys. Rev.* B11, 4152 (1975).
[34] Stanley, H.E., *Introduction to Phase Transitions and Critical Phenomena* (Oxford University Press, Oxford 1971).
[35] Kramers H.A. and Wannier G.H., *Phys. Rev.* 60, 252 (1941).
[36] Domb C. in *Phase Transitions and Critical phenomena*, ed. by C. Domb and M. S. Green, Academic Press, Ney York, 1975, vol. 5, Chap.VI.
[37] Gaunt D.S. and Fisher I.G., *J. Chem. Phys.* 43, 2840 (1965).
[38] Runnels L.K. and Coombs L.L., *J. Chem. Phys.* 45, 2482 (1966).
[39] Runnels L.K., Coombs L.L., Salvant J.P., *J. Chem. Phys.* 47, 4015 (1965).
[40] Baxter R.J., Enting I.G., Tsang S.K., *J. Stat. Phys.* 22, 465 (1980).
[41] Baxter R.J., *Annals of Combinatorics* 3, 191 (1999).
[42] Fisher M.E., *Proc. Roy. Soc. (London)*, A254, 66 (1960).
[43] Bienenstock A. and Lewis J., *Phys.Rev.*, 160, 393 (1967).
[44] Müller-Hartmann E. and Zittartz J., *Z. Physik* B27, 261 (1977).
[45] Yang C.N., *Phys. Rev.* 85, 808 (1952).
[46] LeClaire A.D. in *Physical Chemistry – An Advanced Treatise*, Eds. H. Eyring, D. Henderson and W. Jost, Academic Press Ney York, 1970, v. 10.

CURRICULA VITAE

Alexander Tarasenko. was born in Ukraine in 1950. After graduation (with an award) from Department of Physics, Kyiv National University in 1972, was employed in the Department of Adsorption Phenomena in the Institute of Physics (Academy of Sciences, Kyiv, Ukraine). He obtained his Ph.D. in physics in 1979. Next he worked in the Institute of Physics as a scientific researcher. Main area of his scientific interests includes fluctuation phenomena and plasma instabilities in semiconductors, statistical theory of solid surfaces, phase transitions and kinetic phenomena of low dimensional lattice gas systems. Now he is involved in several projects aiming at theoretical description of diffusion of particles adsorbed on solid surfaces, mechanical properties of films, computer simulations of kinetic phenomena and phase transitions in adsorbed layers. Closely cooperates with scientists from the Institute of Physics (Academy of Sciences, Prague, Czech Republic), University of San Luis (San Luis, Argentina), Max-Planck-Institut fur Eisenforschung (Dusseldorf, Germany). He has published over 70 scientific papers in international journals and has written a book "*Fluctuation phenomena in the bulk and surfaces of solids*" (Naukova dumka, 1992, Kyiv, in Russian) with P. M. Tomchuk and A. A. Chumak. At present he is a member of the Optic Division in the Institute of Physics, Academy of Sciences, Prague, Czech Republic.

Dr. Lubomir Jastrabik was born on July 29, 1944 in Smolenice, Slovakia. He graduated from the Charles University in Prague, Faculty of Mathematics and Physics in 1972. Received his RNDr.(Doctor of natural sciences) degree at the same University in 1975. In 1985 he received Ph.D. degree in solid state physics from the Institute of Physics, Czechoslovak Academy of Sciences, Prague. He was employed in the Institute of Physics, Academy of Sciences of the Czech Republic as a research scientist from 1972 till 1985, as a Head of the Technological Laboratory from 1985 till 1990 and since 1990 hold the position of the Head of the Department of Multilayer Structures. Main field of research: Surface diffusion, phase transitions, optical and dielectric properties, ESR spectroscopy of crystals and thin films. Technologies of preparation of thin films (magnetron spattering, plasma-jet deposition, PE CVD, pulsed laser and ECR microwave plasma deposition), plasma diagnostics. He published over 200 publications in scientific journals and more than 70 papers in conference proceedings.